



ELECTRON BEAM WELDING OF THICK-WALL SHELLS OF ALUMINIUM AMg6 AND M40 ALLOYS

E.G. TERNOVOJ and A.A. BONDAREV

E.O. Paton Electric Welding Institute, NASU, Kiev, Ukraine

Results of investigations on EBW of 40–90 mm thick semi-finished products of aluminium alloys AMg6 and M40 are given. Optimal welding parameters were selected. Properties, microstructural peculiarities and hardness of the resulting joints were studied for horizontal and vertical welds. The EBW technology in fabrication of large-size thick-walled shells of aluminium alloys was developed and passed the industrial testing.

Keywords: electron beam welding, aluminium alloys, shells, longitudinal and circumferential joints, welding conditions, joint properties, hardness, microstructure, industrial testing

The comparison of technological capabilities of the known methods of fusion welding showed that the most challenging method in manufacture of large-size shells of aluminium alloys of large thicknesses is electron beam welding (EBW) [1, 2]. To obtain the required properties of joints in EBW it is necessary to preset the optimal condition parameters, sizes and geometry of fusion zone, sizes of softening zone, etc. [3–9].

In EBW of AMg6 and M40 alloys the decrease of content of elements with high vapor pressure in weld metal is possible which results in decrease of strength characteristics, formation of porosity and cracks in weld metal and near-weld zone [10–14]. In this case the authors of works [1, 2, 5, 9] recommend horizontal arrangement of electron beam which favors the sufficient decrease of defects in weld metal.

The purpose of this work is the development and industrial testing of EBW technology for circumferential and longitudinal butts of shells of aluminium AMg6 and M40 alloys of 40–90 mm thickness, providing preset sizes of fusion zone, formation of two-side reinforcement bead and high properties of joints across the whole thickness of a butt.

During selection of condition parameters, level of deepening of focal spot and working distance for maximum penetration, welding of specimens of AMg6 and M40 alloys with partial penetration without beam scanning was performed. The length of specimens was 500 mm, thickness – 40 mm. The specimens were welded from power source ELA 60/60 in the installation UL-179 at residual pressure in the chamber of $1.33 \cdot 10^{-3}$ Pa. The welding speed was set constant at all conditions and equal to 36 m/h. Basing on carried out experiments the working distance of 220 mm was selected at deepening of focal spot from –10 to +20 mm.

The optimization of welding conditions with through penetration was performed on the plates of AMg6 alloy of $500 \times 200 \times 40$ mm size at the welding speed of 18–85 m/h by a beam without deflections and scanning beam of horizontal and vertical upward welds. The beam current depending on speed of welding varies in the range of 130–275 mA.

During welding of specimens of butt joints the technological circular and transverse scans, as well as discrete scans with adjustable time of delay of beam in the spots of its interruptions were applied [15, 16]. The trajectories of scanning were selected in a form of different curves of the second order (circle, semi-circle, ellipse, semi-ellipse) and their combination with longitudinal or transverse scanning (Figure 1), and shape and parameters were controlled using oscillograph S1-83. Independently of type of scanning or correlation of time of delays of beam on the trajectory of scanning, the amplitude of scanning across the butt was tried to be unchanged in welding of the same thickness in all technological variants and all spatial positions of joints (Figure 2). The conditions of welding of butt joints of AMg6 and M40 alloys and their macrosections are given in Table 1.

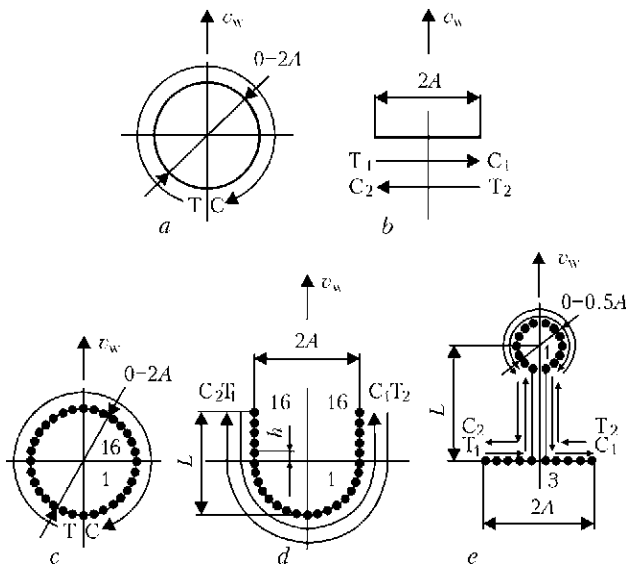





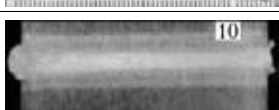




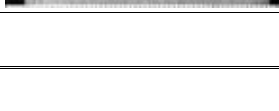


Figure 1. Shapes and trajectories of scans applied in welding of specimens of aluminium alloys: *a, b* – circular and transverse continuous scanning; *c–e* – discrete scanning; *A* – scanning amplitude; *h* – pitch of discrete movement; 1 (minimal), 16 (maximal) and 3 – areas of front and rear fronts of weld pool with corresponding heat input



Table 1. Conditions of welding of upwards vertical and horizontal welds on plates of AMg6 and M40 alloys by horizontal beam

Number of experiment	Alloy	Spatial position of butt welding	Thickness of plates, mm	Beam current, mA	Focusing current, mA	Welding speed, m/h	Macrosection
1	AMg6	Horizontal	40	220	865	30	
2		Vertical upwards	60	275	895	20	
3		Same	90	330	915	12	
4*		Horizontal	90	330	915	12	
5*	M40	Vertical upwards	40	395	870	45	
8		Horizontal	40	395	870	45	
9		Vertical upwards	50	365	822	25	
10		Same	50	465	902	30	
11		»	50	365	870	36	
12		»	50	495	902	45	
13		Horizontal	65	630	915	36	

*Welding using scanning beam with a circular scan.

The evaluation of quality of welded joints was performed applying 100 % control of density of joints using X-ray method, measuring of geometric sizes of penetration zone and HAZ on transverse sections, determining the composition of weld metal according to base alloying components using method of local spectral analysis, investigating the microstructure of different zones of welded joints and distribution of hardness, determining the strength characteristics of joints and their scattering across the thickness of billets.

The X-ray control of joints did not detect any large defects in a form of pores, cracks, lacks of penetration or voids in welds.

While producing horizontal welds on the plate of AMg6 alloy the clearly distinct structural heterogeneity across the weld section is observed, especially in its lower part (Figure 3). The presence of practically continuous chain of secondary phase precipitates across the layers of crystallization (Figure 3, c) results in considerable anisotropy of properties across the section of a butt and large discrepancy of their values in the range of one batch of specimens being tested. While producing vertical upward joints of plates of M40 alloy the defects in a form of non-fused hollows closer to root weld and also microdefects in HAZ metal in a form of low-melting intergranular layers,

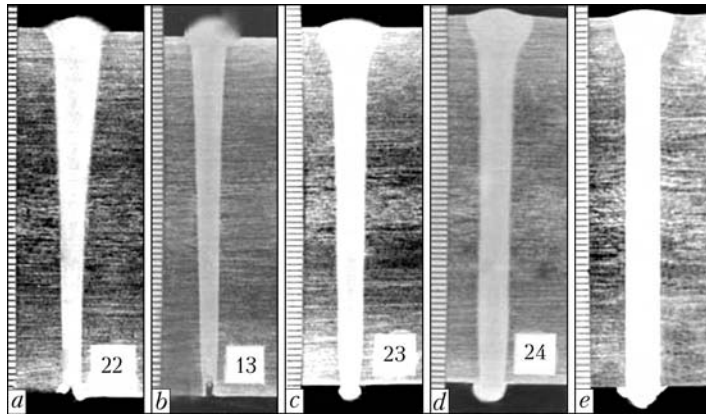


Figure 2. Macrosections of butt joints of AMg6 alloy of 60 mm thickness produced using scanning: *a, b* – respectively, continuous circular and transverse scanning; *c* – discrete circular scanning; *d* – discrete U-shape scanning; *e* – discrete combined scanning (circle with transverse scanning); *a, d* – welding using horizontal beam on the vertical plane; *b, c, e* – welding upwards using horizontal beam

coagulated inclusions and preliminary fused eutectic phases facilitating formation of single micropores and porosity resulting in decrease of impact toughness along the fusion boundary are possible. The coefficient of strength decreases to the level of $0.85\sigma_t$ of base metal.

The processing and analysis of results of evaluation of joints of AMg6 and M40 alloys with parallel boundaries of penetration zone prove that in this case the stable weld formation across the whole depth independently of thickness of semi-products at welds width of 5–8 mm and double-sided formation of reinforcement beads (macrosections in Table 1) is achieved. In addition in the course of mechanical tests of joints their high properties were established and metallographic examinations of weld metal and HAZ showed that using this method the sizes of grains in upper, middle and root parts of weld metal are refined and stabilized, the content of hydrogen and thickness of precipitates in intergranular layers are reduced, HAZ sizes are decreased.

The chemical compositions of base and weld metal of produced joints of AMg6 (thickness of 40, 60 and 90 mm) and M40 (thickness of 40, 50 and 65 mm) alloys appeared to be identical for all thicknesses. Thus, AMg6 alloy contains (wt.%): 6.65–6.75 Mg;

0.55–0.59 Mn; Al – base, and alloy M40 contains 5.0 Cu; 3.60–3.70 Mg; 0.43 Mn; Al – base. The losses of magnesium for evaporation in weld metal did not exceed 0.02–0.04 %.

The results of mechanical tests of produced welded joints of AMg6 and M40 alloys for all thicknesses evidence (Tables 2 and 3) that joints are characterized by high stability of values of ultimate tensile strength and impact toughness, whereas heterogeneity of properties across the whole thickness of the butt is practically absent. The most peculiar feature is that the impact toughness of joints with Charpy notch across the middle of the weld is by 15–20 % higher than that in base metal and preserved almost at the same level when the notch along the fusion boundary was performed.

The analysis of microstructure of joints of AMg6 alloy detected by reagent of Keller showed that except the α -solid solution of magnesium and manganese, there are double and more complicated phases in aluminium, arranged in the form of thin, sometimes continuous chains along the grain boundaries in the base metal and between branches of dendrites in a weld metal (Figure 4). In the lower part of joints, due to the higher rates of solidification, the central dendrites

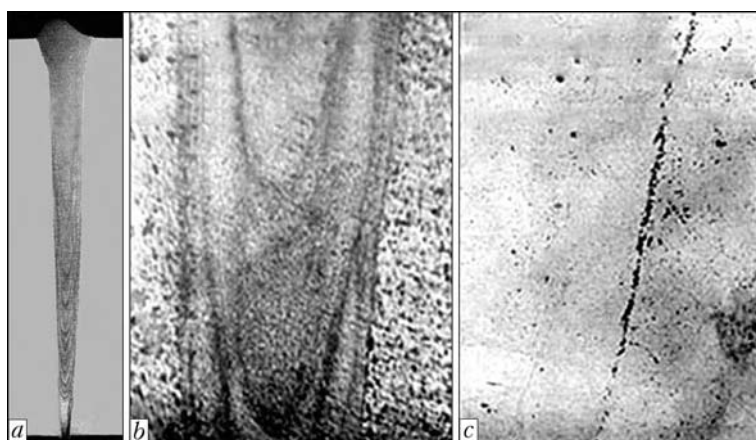


Figure 3. Lamellar structural heterogeneity in weld on AMg6 alloy of 90 mm thickness produced by EBW with circular scanning: *a* – macrosection of joint; *b* – macrostructure ($\times 20$) of joint in the lower part of weld; *c* – microstructure ($\times 300$) of weld at the area of secondary phase precipitation



Table 2. Mechanical properties of base metal and EB-welded joints of plates of AMg6 alloy

Number of specimen	Thickness of BM and butt, mm	σ_t , MPa	KCV, J/cm ²		Object of testing
			Notch across the weld middle	Notch along the weld boundary	
1	40	$\frac{350-355}{360}$	$\frac{22-25}{23}$	–	BM, upper part
2*		$\frac{262-309}{280}$	$\frac{20-21}{20}$	$\frac{12-15}{14}$	Butt joint, defects in a form of holes
3*		$\frac{313-324}{324}$	$\frac{23-26}{25}$	$\frac{15-17}{16}$	Butt joint, laminar heterogeneity
4		$\frac{345-350}{348}$	$\frac{27-29}{28}$	$\frac{18-22}{20}$	Butt joint
5	60	$\frac{346-352}{350}$	$\frac{18-19}{18}$	–	BM
6		$\frac{335-340}{340}$	$\frac{25-27}{27}$	$\frac{18-22}{21}$	Butt joint
7	90	$\frac{342-354}{350}$	$\frac{18-19}{19}$	–	BM
8		$\frac{335-338}{336}$	$\frac{22-25}{23}$	$\frac{17-19}{19}$	Butt joint

*Welding by circular scanning beam.

Table 3. Mechanical properties of base metal and EB-welded joints of plates of M40 alloy

Number of specimen	Thickness of BM and butt, mm	σ_t , MPa	KCV, J/cm ²		Object of testing
			Notch across the weld middle	Notch across the weld boundary	
1	40	$\frac{400-415}{400}$	$\frac{9.7-11.0}{10.8}$	–	BM
2*		$\frac{313-322}{320}$	$\frac{3-6}{5}$	$\frac{5.0-5.6}{5.0}$	Butt joint
3		$\frac{388-392}{390}$	$\frac{5.1-6.2}{5.3}$	$\frac{6.8-7.2}{7.0}$	Same
4	50	$\frac{410-420}{415}$	$\frac{9.8-11.5}{10.5}$	–	BM
5		$\frac{365-375}{370}$	$\frac{7.6-8.5}{7.9}$	$\frac{6.9-7.8}{7.1}$	Butt joint

*Welding by circular scanning beam.

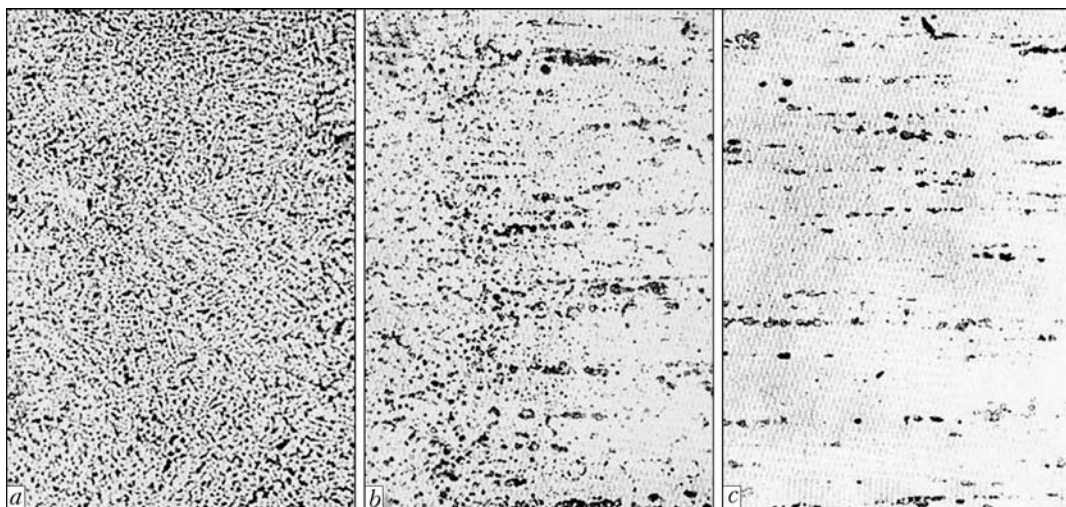


Figure 4. Microstructure ($\times 160$) of characteristic zones of welded joint of AMg6 alloy of 40 mm thickness: *a* – weld metal; *b* – fusion zone; *c* – base metal



HRB

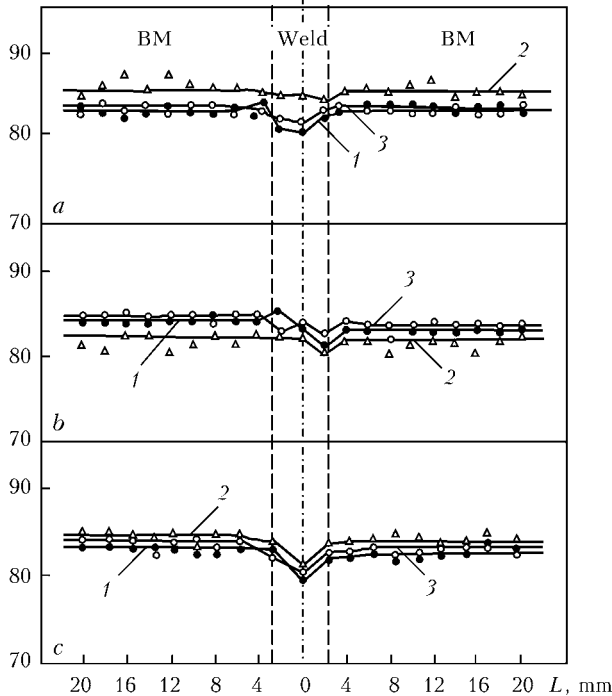


Figure 5. Distribution of hardness across the EB-welded joints of AMg6 alloy 90 mm thick (rolled metal): *a-c* – levels of hardness measurements at the distance from the plate surface on the side of beam input are 10, 45, 80 mm, respectively; 1 – continuous circular scanning (butt); 2, 3 – discrete scanning (2 – penetration; 3 – butt)

are formed with more branched structure as compared to the structure of upper part of a butt. There are no defects in fusion zone except of single micropores.

During measurement of hardness of welded joints of AMg6 alloy of 90 mm thickness using Rockwell device with a ball of 1 mm at loading of 600 N at three levels along the section of a butt, the considerable decrease in hardness of base metal (*HRB* 82–84) up to the fusion boundary was not observed. In the upper part of a butt the hardness of weld metal is *HRB* 80 and is insufficiently increased up to *HRB* 82–83 in the middle part of a weld, and closer to reverse bead the hardness is decreased to *HRB* 79–80

HRB

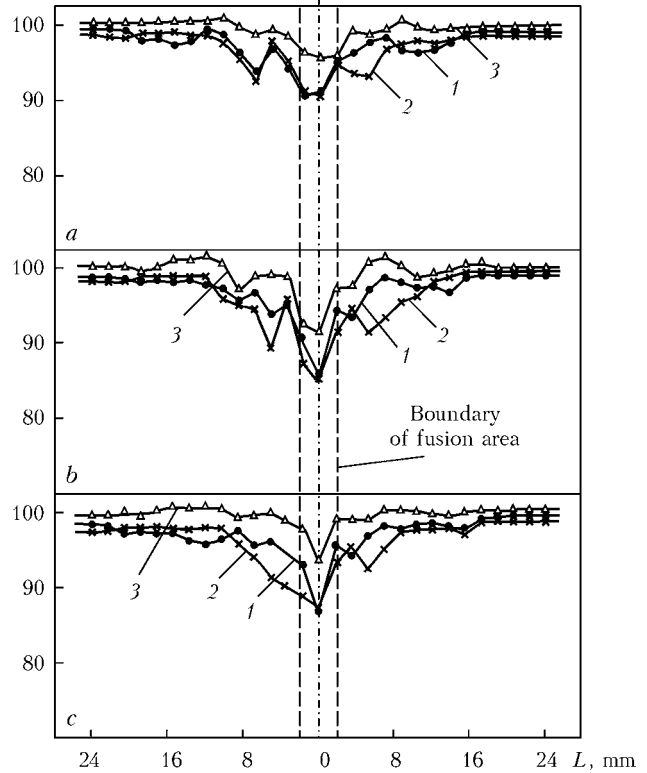


Figure 6. Distribution of hardness in EB-welded joints of M40 alloys 50 mm thick: 1–3 – the same as in Figure 5

(Figure 5). The selection of optimal welding conditions of butt joints for M40 alloy was performed on plates of 50 mm thickness at the speeds of 25, 30, 36 and 45 m/h (see Table 1). The measurement results of hardness are shown in Figure 6. From the Figure it is seen that decrease in welding speed from 45 to 25 m/h results in increase of HAZ (from 9 to 13 mm to one side, including a weld), but it does not almost change a hardness of weld metal at all levels of measurements. In addition using heat treatment (artificial ageing) the hardness of weld metal can be increased. The influence of welding speed on microstructure of weld and near-weld zone showed that decrease of welding speed makes weld structure and eutectic in-

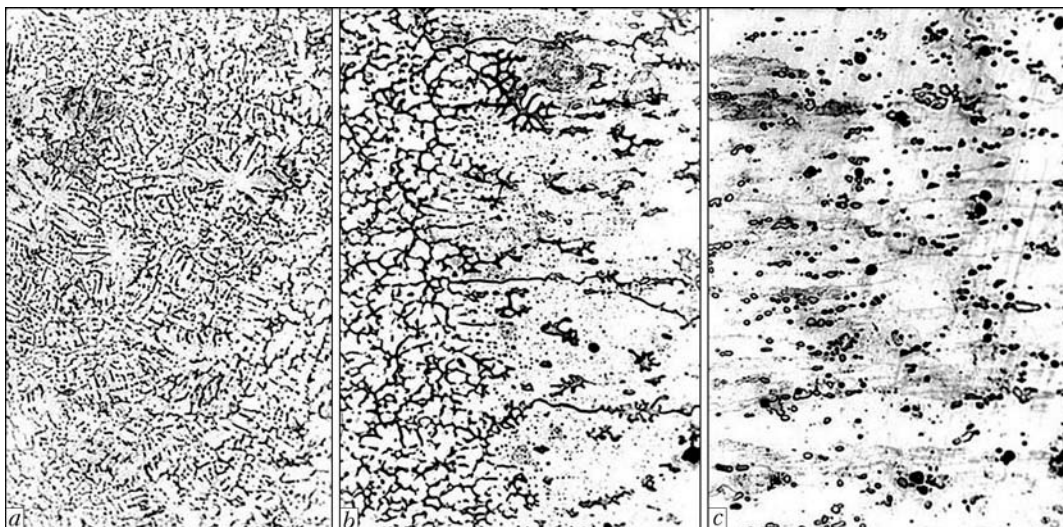


Figure 7. Microstructures ($\times 160$) of different zones of welded joint of M40 alloy 50 mm thick: *a* – weld metal; *b* – fusion zone; *c* – base metal

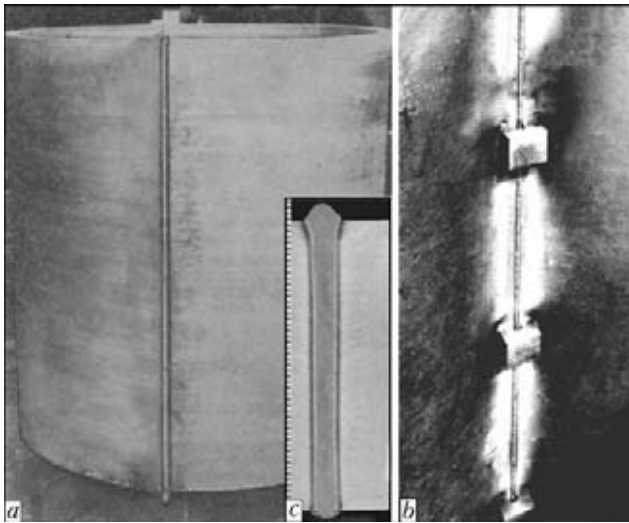


Figure 8. Appearance of welded shell of M40 alloy (a), reversed bead of longitudinal weld (b) and microsection of joint (c)

terlayers in HAZ metal coarser, though the weld structure remains rather fine-dispersed and uniaxial. The influence of welding speed on recrystallization of base metal was studied. The metallographic analysis showed that area of base metal recrystallization in welding at the speed of 25 m/h does not exceed 4 mm. The microstructure of weld and near-weld zone for butt joint of M40 alloy of 50 mm thickness produced at the speed of 45 m/h is given in Figure 7. As is seen, the decrease of welding speed to 25 m/h does not influence the change of weld metal composition. However, the softening along the fusion boundary and decrease of impact toughness by 2 times as compared to base metal are observed. The increase of welding speed to 45 m/h and artificial ageing of welded joints allowed increasing the impact toughness in HAZ to 20 % as compared to that at 25 m/h.

As a result of carried out works on EBW semi-finished products of aluminium AMg6 and M40 alloys, the industrial testing of technology of welding the shells with circumferential and longitudinal joints of 40, 50, 60, 65 and 90 mm thickness was developed and carried out at the PA «Strela» (Orenburg, RF). In Figure 8 the shell with outside diameter of 1250 mm, height of 1500 mm and wall thickness of 50 mm of sheet rolled metal of M40 alloy with longitudinal butt joint produced by EBW is shown, and in Figure 9 – shell with inner diameter of 800 mm, height of 1700 mm and thickness of walls of 40, 60 and 90 mm with circumferential butt joints, made of AMg6 alloy forgings.



Figure 9. Appearance of welded shell with changeable thickness of wall made of AMg6 alloy forgings (a), and macrosection of joint (b)

1. Bondarev, A.A. (1980) EBW, its advantages and main principles in development of welding technology of aluminium alloys. In: *Proc. of 1st All-Union Conf. on Welding of Light, Nonferrous and Refractory Metals and Alloys* (Kiev, 21–23 Nov., 1978). Kiev: Naukova Dumka, 106–110.
2. Bondarev, A.A. (1984) State-of-the-art and advantages of electron beam welding process of aluminium alloy structures. In: *Proc. of Soviet-American Seminar on Welding of Aluminium Alloys of Cryogenic and General Purposes* (Tashkent, 17 Oct. 1982). Kiev: Naukova Dumka, 10–19.
3. Olshansky, N.A., Khokhlovsky, A.S., Balayan, R.F. et al. (1985) Properties of welded joints of large thickness aluminium and magnesium alloys made by EBW. In: *Proc. of 2nd All-Union Conf. on Welding of Light, Nonferrous and Refractory Metals and Alloys* (Tashkent, 17 Oct. 1982). Kiev: Naukova Dumka, 164–166.
4. Pisarsky, V.I. (1977) EBW of large thickness aluminium alloys. In: *Proc. of All-Union Conf. on EBW* (Kiev, 17–29 Oct. 1975). Kiev: Naukova Dumka, 168–171.
5. Bondarev, A.A., Tretyak, N.G., Kuzmenok, O.S. et al. (1978) Technology of EBW of large-sized structures of AMg6 alloy. *Avtomatich. Svarka*, **9**, 54–56.
6. Bondarev, A.A., Tretyak, N.G. (1980) Influence of parameters on sizes of penetration zone and joint properties in electron beam welding of alloy 1201 plates. In: *Proc. of 1st All-Union Conf. on Welding of Light, Nonferrous and Refractory Metals and Alloys* (Kiev, 21–23 Nov. 1978). Kiev: Naukova Dumka, 114–117.
7. Nazarenko, O.K., Kajdalov, A.A., Kovbasenko, S.N. et al. (1987) *Electron beam welding*. Kiev: Naukova Dumka.
8. Khokhlovsky, A.S., Yakhontov, S.A. (1980) Effect of hydrodynamic processes in penetration channel on EBW joints of light alloys. *Trudy MEI*, **475**, 9–21.
9. Voropaj, N.M., Bondarev, A.A., Ivanov, N.P. et al. (1972) Development of EBW technology of product bodies of AMg6 alloy. *Svarochn. Proizvodstvo*, **3**, 18–20.
10. Bondarev, A.A., Voropaj, N.M., Rabkin, D.M. et al. (1972) EBW of aluminium alloy spherical vessels. *Avtomatich. Svarka*, **5**, 44–47.
11. Zajtsev, V.I., Skorospelov, V.V. (1980) Experience in fabrication of welded vessels of heat-resistant aluminium alloy M40. In: *Proc. of 1st All-Union Conf. on Welding of Light, Non-Ferrous and Refractory Metals and Alloys* (Kiev, 21–23 Nov. 1978). Kiev: Naukova Dumka, 76–81.
12. Ishchenko, A.Ya., Ignatiev, V.G., Chayun, A.G. et al. (1979) Weldability of aluminium alloy M40. *Avtomatich. Svarka*, **10**, 15–18.
13. Bondarev, A.A., Rabkin, D.M. (1974) Evaporation of volatile elements in EBW of aluminium alloys. *Ibid.*, **3**, 13–16.
14. Detsik, N.N. (1980) Peculiarities of evaporation of weld alloyed elements in intermediate vacuum EBW. *Elektrotekh. Promyshlennost. Series Electric Welding. Issue 4*, 1–4.
15. Bondarev, A.A., Skryabinsky, V.V. (1987) Welding of aluminium alloys with programming of electron beam density distribution by heating spot. In: *Automatic control of technological process of electron beam welding*. Kiev: PWI.
16. Lankin, Yu.N., Bondarev, A.A., Dovgodko, E.I. et al. (2009) Control system for beam scanning in electron beam welding. *The Paton Welding J.*, **9**, 13–16.